Journal of Oceanology and Limnology
Vol. 38 No. 1, P. 102-113, 2020
https://doi.org/10.1007/s00343-019-8357-9

Integrated transcriptome and physiology analysis of *Microcystis aeruginosa* after exposure to copper sulfate*

WANG Tao[1, 2, 4], HU Yadong[1], ZHU Ming[3, 4], YIN Shaowu[1, 2, **]

[1] *College of Marine Science and Engineering*, *College of Life Science*, *Nanjing Normal University*, *Nanjing 210023*, *China*
[2] *Co-Innovation Center for Marine Bio-Industry Technology of Jiangsu Province*, *Lianyungang 222005*, *China*
[3] *College of Marine Life and Mariculture*, *Huaihai Institute of Technology*, *Lianyungang 222005*, *China*
[4] *Nanjing Ocean-wisdom Biotech Company*, *Nanjing 211132*, *China*

Received Dec. 17, 2018; accepted in principle Mar. 18, 2019; accepted for publication Apr. 15, 2019

Abstract Copper sulfate ($CuSO_4$) is widely used in controlling the *Microcystis aeruginosa* blooms. Many studies reported the toxicity mechanisms of Cu^{2+} to *M. aeruginosa* at the physiological level, but little is known about a transcriptomic basis of these mechanisms. In the present study, *M. aeruginosa* was treated by 0.5 mg/L Cu^{2+} (half of the 96-h EC_{50}) for 72 h. The results show that Cu^{2+} content in *M. aeruginosa* increased after 72 h Cu^{2+} exposure, whereas the F_v/F_m chlorophyll fluorescence value and chlorophyll *a* content in *M. aeruginosa* sharply decreased. Reactive oxygen species concentration and activity of antioxidant enzymes (superoxide dismutase, catalase and peroxidase) were all increased. These physiological data confirmed toxicity of Cu^{2+} to *M. aeruginosa*. The RNA-seq analysis showed that 6 646 725 and 7 880 291 clean reads were obtained for the Cu-treated and control libraries, respectively. The 595 genes (252 downward trend and 343 upward trend) with the Gene Ontology (GO) annotations were divided into three main functional categories: cellular component, molecular function, and biological process. In the Cluster of Orthologous Groups (COG) annotation, 418 differentially expressed genes with 25 functional definitions were obtained. Among them, 'replication, recombination and repair', 'energy production and conversion', and 'general function prediction only' were the largest three groups of transcripts. In the Kyoto Encyclopedia of Genes and Genomes (KEGG) pathway analysis, genes involved in photosynthesis and oxidative phosphorylation were present at the highest percentages. In addition, the genes involved in photosynthesis and oxidative phosphorylation were identified, and then confirmed using real-time PCR. This study reported the first transcriptome of *M. aeruginosa*. Photosynthesis and oxidative phosphorylation were severely affected by Cu^{2+} toxicity, which may have contributed to cell death. These data provide the potential mechanism to explain the $CuSO_4$ effect on the harmful *M. aeruginosa*.

Keyword: transcriptome; physiology; *Microcystis aeruginosa*; copper sulfate

1 INTRODUCTION

As a result of global temperature and eutrophication, the *Microcystis aeruginosa* blooms are increasing in the freshwater ecosystems, becoming a global environmental problem (Wu et al., 2017). The direct effects of the mass growth of *M. aeruginosa* are unpleasant odor, loss of water transparency, and depletion of oxygen. This species produces microcystins (potent hepatotoxins to aquatic and terrestrial animals) that threaten public health regarding drinking water supply and recreational activities such as fishing (Otten and Paerl, 2015).

Many available methods tried to prevent the occurrence of blooms, including physical, chemical, and biological ways. One such a method is to reduce nutrient input into water systems to prevent nutrient enrichment and favor phytoplankton rather than

* Supported by the Natural Science Foundation of Jiangsu Province of China (No. BK20180728), the Key Research and Development Program of Jiangsu Province (No. BE2017377), and the Creation Project of Major New Species of Agriculture in Jiangsu Province (No. PZCZ201742)
** Corresponding author: yinshaowu@163.com

cyanobacteria (Hrudey et al., 1999; Otten and Paerl, 2015), but this method is not particularly successful. Using chemical agents to inhibit or kill cyanobacteria may support ecological restoration and control the occurrence of blooms (Barrington and Ghadouani, 2008). Although the chemical methods may have serious negative impacts on the ecosystem, it has so far been considered an effective strategy to control *M. aeruginosa* blooms (Zhou et al., 2013; Wu et al., 2017).

At present, copper sulfate ($CuSO_4$) is a low-cost chemical reagent used to inhibit *M. aeruginosa* blooms, on which many papers have been published documenting toxicity of Cu^{2+} to *Microcystis* (Hadjoudja et al., 2009; Wu et al., 2017). Leng et al. (2015) reported that Cu^{2+} could cause rapid and excessive accumulation of reactive oxygen species (ROS) in *M. aeruginosa* and disrupt membrane integrity. Rascioa and Navari-Izzo (2011) suggested that the Cu^{2+} toxicity to plants might be caused by inactivating enzymes, blocking of functional groups of metabolically important molecules, and/or displacing or substituting for essential elements in numerous physiological processes. However, to the best of our knowledge, the published materials did not address the mechanisms of Cu^{2+} toxicity to *M. aeruginosa* from a transcriptome perspective. Presently, availability of complete *M. aeruginosa* genome and high-throughput RNA sequencing (RNA-seq) techniques offer tools for the study on the mechanisms of Cu-dependent stress response in *M. aeruginosa* (Kaneko et al., 2007; Wang et al., 2017).

A moderate dose of $CuSO_4$ can be used to inhibit the growth of *Microcystis* and control bloom formation, which is non-toxic to humans and aquatic animals (Zhang et al., 2007; Barrington and Ghadouani, 2008). Tsai (2015) reported that Cu^{2+} concentration of 0.16 mg/L is the minimum concentration required to inhibit the growth of *M. aeruginosa*. Zhang et al. (2007) found the 96-h EC_{50} of *M. aeruginosa* was 1.02 mg/L Cu^{2+}. The Cu^{2+} doses below 2 mg/L are considered safe according to the World Health Organization recommendation.

In this study, *M. aeruginosa* was treated in 0.5 mg/L Cu^{2+} (half of the 96-h EC_{50} according to Zhang et al., 2007) for 72 h. We characterized the toxicological effects of Cu^{2+} at a physiological level. The goals of this study are to construct a *M. aeruginosa* transcriptome database, to screen the significantly expressed genes under Cu-toxic conditions, to understand Cu^{2+} toxicity mechanism in *M. aeruginosa*, and to provide a genetic resource of *M. aeruginosa*.

2 MATERIAL AND METHOD

2.1 *M. aeruginosa* culture and Cu^{2+} treatment

Microcystis aeruginosa was purchased from the Institute of Hydrobiology, Chinese Academy of Sciences. *M. aeruginosa* were cultured at 28°C under 2 500-lx lighting in 12 h/12 h light/dark cycle in BG-11 medium. The initial concentration of *M. aeruginosa* in both the control and the treatment was 10^6 cells/mL, and 0.5 mg Cu^{2+} (as $CuSO_4$) per liter was added to the treatment group; the study lasted for 72 h. Each treatment was replicated three times. In this experiment, we aimed to monitor the Cu^{2+} stress responses rather than the algae death, so that the treatment of Cu^{2+} concentration was chosen carefully. In previous experiments, we found that 0.5 mg/L Cu^{2+} was the appropriate concentration, resulting in a sharp decline in several physiological traits, while the mortality of *M. aeruginosa* was below 20%.

2.2 Biochemical analysis

Photosynthetic efficiency was evaluated by using a handy photosynthetic efficiency analyzer (Handy-PEA, Hansatech Instruments Ltd, Norfolk, UK). Parameters F_v (variation in fluorescence) and F_m (maximal fluorescence in the dark-adapted state) were measured at 0, 24, 48, and 72 h after commencement of the Cu^{2+} treatment. Subsequently, the value of F_v/F_m was calculated.

The ROS concentration was measured at 0, 24, 48, and 72 h according to Guo et al. (2016a) after staining the cells by DHR123 (dihydrorhodamine 123) for 1 h. The final concentration of DHR123 in the cell cultures was 5 μmol/L. After incubation, fluorescence (for excitation/emission at a wavelength of 485/530 nm) was measured using a fluorescence spectrophotometer (Model LS-55, PerkinElmer, CA, USA) to quantify the ROS concentration.

At the end of the experiment, chlorophyll *a* (Chl *a*) concentration was determined at room temperature using a PHYTO-PAM phytoplankton analyzer (Water-PAM, Walz, Germany). This was performed after keeping the cells in the dark for 7.5 min prior to measurement based on the published method (Gera et al., 2012)

Copper concentration in *M. aeruginosa* was measured as per Foster et al. (2008). Briefly, approximately 50.0 mg freeze-dried algal sample was digested with 2 mL HNO_3 at 120°C. Total Cu^{2+} was determined by inductively coupled plasma-

optical emission spectroscopy (ICP-OES, Optima 7000, PerkinElmer, USA).

Antioxidant enzyme activities were measured using the commercial kits (purchased from Nanjing Jiancheng Bioengineering Research Institute of China, Nanjing, China) (Gui et al., 2010). The total superoxide dismutase (SOD) assay was based on the SOD-mediated inhibition of nitrite formation from hydroxylammonium in the presence of an O_2^- generator (Hong et al., 2008). The catalase (CAT) activity was defined as the amount of enzyme required to transform 1-μmol H_2O_2/min at 28°C and pH 7.0. The peroxidase (POD) activity was defined as a 0.01-absorbance unit change per min at 470 nm. The malondialdehyde (MDA) content was measured based on the chemical reaction between MDA and 2-thiobarbituric acid (TBA), which is expressed as nmol MDA/mg protein (Ohkawa et al., 1979). Total soluble protein was measured using the Bradford method (Bradford, 1976).

2.3 Transcriptome analysis

2.3.1 RNA extraction, cDNA library construction and Illumina deep sequencing

Total RNA samples of Cu^{2+}-treated and control group were extracted using commercial kits (Trizol reagent, Invitrogen, USA), and subsequently used for mRNA purification and library construction following the manufacturer's instructions (the Ultra RNA library prep kit for Illumina, NEB, USA). Then, the samples were sequenced on an Illumina Hiseq 2500, and each sample yielded >2 Gb of data. Sequencing was completed by the Nanjing Genepioneer Biotechnologies Company (Nanjing, Jiangsu, China). Three repetitions were used for RNA-Sequencing.

2.3.2 Transcriptome data analysis

The procedure of transcriptome data analysis was as follows. Firstly, low quality reads and reads containing adapter or ploy-N were removed from the raw data, generating the high-quality clean data. Secondly, the clean reads were mapped to the *M. aeruginosa* NIES-843 genome. Thirdly, the numbers of reads mapping to each gene were counted, and FPKM of each transcript was calculated according to the published method (Trapnell et al., 2010). Fourthly, differential expression genes (DEGs) were analyzed by the DESeq R package (Anders and Huber, 2010). The significant DEGs among different samples were identified with $P<0.05$ and log2 fold-change >1. Finally, we used the GOseq R package, COGPipeline and KOBAS software to implement, respectively, the Gene Ontology (GO), Cluster of Orthologous Groups of proteins (COG) and Kyoto Encyclopedia of Genes and Genomes (KEGG) enrichment analyses of DEGs. In our study, the degree of KEGG enrichment was measured using the Richfactor, *Q*-value, and the number of genes enriched in a KEGG pathway. The Richfactor refers to the ratio of the number of differentially expressed to the total number of annotated genes. The larger the Richfactor value, the greater the degree of enrichment. The *Q*-value is the *P*-value after multi-hypotheses test correction in a range of 0–0.05; the closer the value is to zero, the more significant the enrichment (Wang et al., 2018).

2.4 Real-time PCR

Purified RNA was reverse-transcribed into cDNA using a First Strand cDNA Synthesis Kit according to the manufacturer's instructions (TaKaRa, Japan). To adjust the quantity of input cDNA, *16S rRNA* was used as the internal control (Chen et al., 2015). The primers (as listed in Table 1) for RT-PCR were designed according to the known sequences of *M. aeruginosa* in National Center for Biotechnology Information (NCBI).

RT-PCR was performed using the SYBR Premix EX Taq (TaKaRa, Japan) on an ABI 7500 Real-Time PCR System. An aliquot of 2.0-μL template cDNA was added to the final volume of 20-μL reaction mixture. The RT-PCR protocol consisted of initial denaturation at 95°C for 30 s, followed by 35 cycles of 95°C for 3 s each, and annealing at 60°C for 34 s. The final dissociation stage included one cycle of 95°C for 15 s, 60°C for 1 min and 95°C for 15 s. In this study, we calculated the relative quantity of the target gene transcripts with respect to the *16S rRNA* (Chen et al., 2015) using the $2^{-\Delta\Delta Ct}$ method.

3 RESULT

3.1 Physiological parameters of *M. aeruginosa*

As shown in Table 2, Cu^{2+} content in *M. aeruginosa* increased after Cu^{2+} exposure for 72 h, while Chl *a* content in *M. aeruginosa* sharply decreased. Activities of antioxidant enzymes (SOD, CAT and POD) and MDA concentration were all increased after the 72-h Cu^{2+} exposure.

Table 1 Sequences of the primer pairs in *M. aeruginosa* for real-time PCR

Target gene	Forward (5′→3′)	Reverse (5′→3′)	Gene ID
psbA	GCGGCAACGATATTGTAGGTTT	TTCGGCGGTTCCTTGTTC	MAE_RS25355
psbD	GTTTGAAGACGGTGAAGG	TGTTGGAGAAAGCGATGC	MAE_RS07875
psaC	CGCACGGAAGACTGTATTGG	CATACTGCGGGTGGTTTCTGCTC	MAE_RS25860
ATPb	ATAAAGAGTTACAGGACATCATCGC	CCACGAAGAAAGGTTGCGAGAGGAA	MAE_RS00390
rbcL	CGTTTCCCCGTCGCTTT	CCGAGTTTGGGTTTGATGGT	MAE_RS20790
ndhC	TGTTTGCCCTCGTTTTCGTGG	CTCCTTTTCGCCAAGCATAGAC	MAE_RS05180
Cyt-c	TCTGTTACGGTCAATGGATT	GGAAGATGGCGACGATAC	MAE_RS09990
SDH	ACGCCTACGATACTGTCA	CACGCCTAGATGTTCCAAT	MAE_RS24490
16S rRNA	CTAAAGGCGGTGGAAACTGG	CGGCTAGGACTACAGGGGTATCT	U03402.1

Table 2 Some physiological parameters of *M. aeruginosa* under Cu^{2+} toxicity stress after 72 h

Physiological and biochemical parameters	Control	$CuSO_4$ treatment	Percent increase (%)
Cu^{2+} contents (μg/g dry weight)	6.2±0.8	90.3±1.9	1 356±160
Chl *a* contents (μg/L)	220.0±5.2	98.8±6.8	-55±1.2
MDA content (nmol/mg protein)	1.5±0.3	4.6±0.4	212±21
SOD activity (U/mg protein)	6.3±0.9	11.2±1.1	79±4.7
CAT activity (U/mg protein)	4.1±0.2	8.1±0.6	97±2.9
POD activity (U/mg protein)	10.4±2.2	20.8±3.1	102±7.6

Means±SE.

Table 3 Sequencing data summary

Parameter	Cu^{2+}-treated library	Control library
Total raw reads	1 994 017 500	2 364 087 300
Total clean reads	6 646 725	7 880 291
≥Q20 percentage (%)	94.9	93.5
≥Q30 percentage (%)	83.7	84.7
GC percentage (%)	45.9	46.1

3.2 Photosynthetic efficiency and ROS accumulation of *M. aeruginosa*

The value of F_v/F_m was decreased in the Cu^{2+} treatment with increasing exposure time (Fig.1a). The cellular ROS production was detected by measuring the specific fluorescence intensity that increased with increasing exposure time in the Cu^{2+} treatment (Fig.1b).

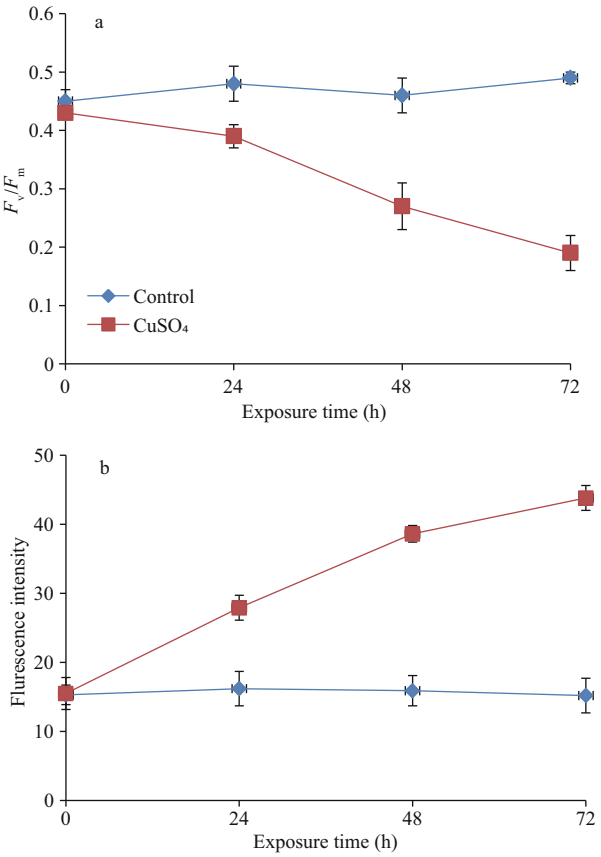

Fig.1 The photosynthetic efficiency (a), and ROS accumulation evaluated by fluorescence intensity of DHR 123 (b)

3.3 Overview of the sequencing

In total, there were 1 994 017 500 raw reads generated from the Cu^{2+}-treated and 2 364 087 300 from the control library (Table 3). After discarding the low quality reads, 6 646 725 and 7 880 91 clean reads were obtained for the Cu^{2+}-treated and control libraries, respectively. Of these clean reads, the Q30 percentage was above 84% and GC content was approximately 46% for the two libraries.

3.4 Functional annotation of the DEGs

For annotation, all DEGs were aligned to databases such as NR, Swiss-Prot, GO, KEGG, and COG by blastx with an *E*-value cut-off of 10^{-5}. The results

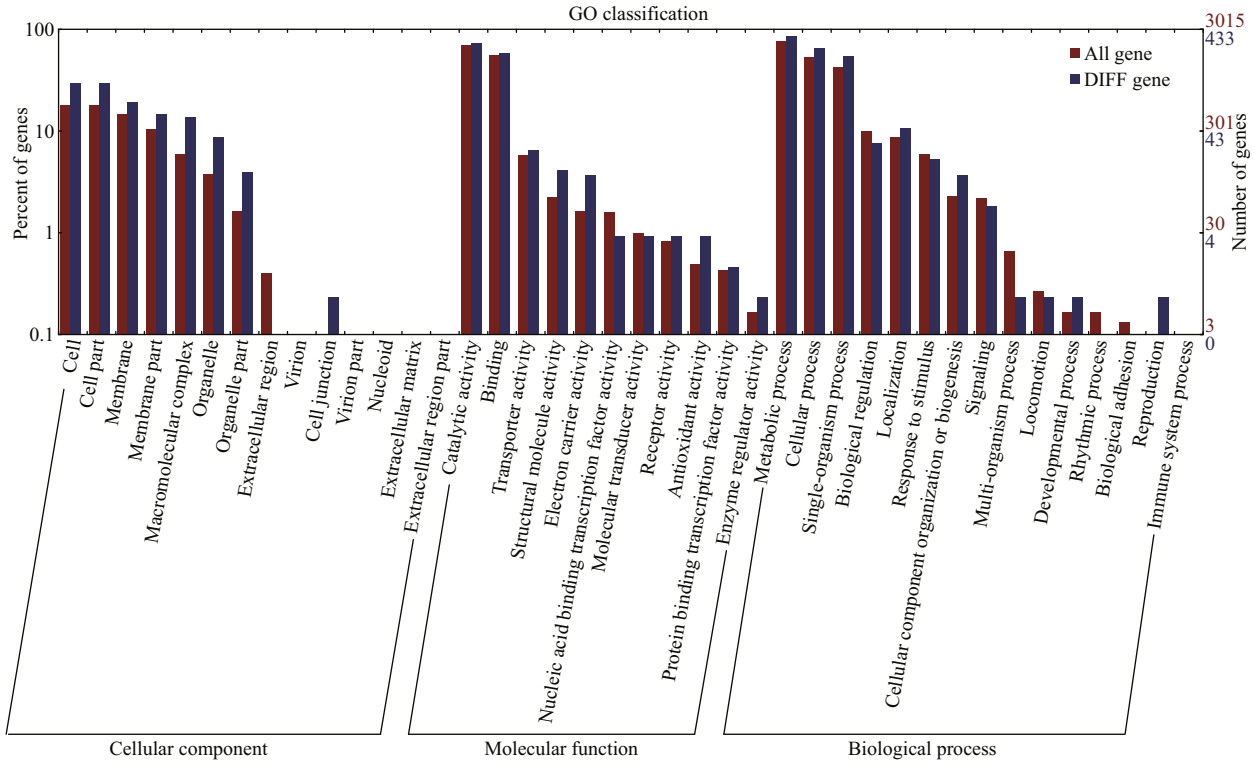

Fig.2 The GO categories of the DEGs

According to the GO terms, the annotated DEGs were classified into the cellular component, molecular function and biological process categories. The right panel shows the gene numbers mapped to the GO terms. The left panel shows the proportions of all genes and different genes according to the GO terms.

Table 4 Overview of functional annotation of the DEGs

DEG set	Total	Swiss-Prot	GO	KEGG	COG	NR
Control vs treatment	594	435	433	292	418	594

indicate that 594 DEGs in the transcriptome libraries were successfully annotated in at least one of the above databases. Specifically, all DEGs were annotated in the NR database, whereas only 292 had the significant matches in KEGG (Table 4).

3.5 Functional classification of transcripts by GO

GO is a useful program for annotating and analyzing the functional categorization of annotated genes (Conesa et al., 2005). The total of 595 genes (343 up-regulated and 252 down-regulated) with the GO annotations were classified into the following three functional categories: cellular component, molecular function and biological process. In the cellular component category, the majority of the annotated DEGs were assigned to cell, cell part, and membrane. In the molecular function category, the widest distribution of the DEGs was associated with catalytic activity and binding. The majority of the DEGs were involved in the metabolic, cellular and single-organism processes in the category biological process (Fig.2).

3.6 Functional classification of transcripts by COG

COG is a database for the classification of orthologous gene products. The COG analysis of the DEGs provided information about their possible functions. The total of 418 DEGs with 25 functional definitions were obtained (Fig.3). Among them, ‘replication, recombination and repair’, ‘energy production and conversion’, and ‘general function prediction only’ were the largest three groups of transcripts.

3.7 KEGG pathway analysis

As shown in Fig.4, the KEGG enrichment analyses of the DEGs showed that the majority were assigned to three specific KEGG categories, including “environmental information processing”, “metabolism” and “genetic information processing”. In addition, the KEGG pathway enrichment analysis showed that, among the top 10 enriched pathway for the Cu^{2+}-treated vs control, the “photosynthesis” and “oxidative phosphorylation” pathway was significantly enriched (with Q-value<0.05 and the largest number of genes enriched).

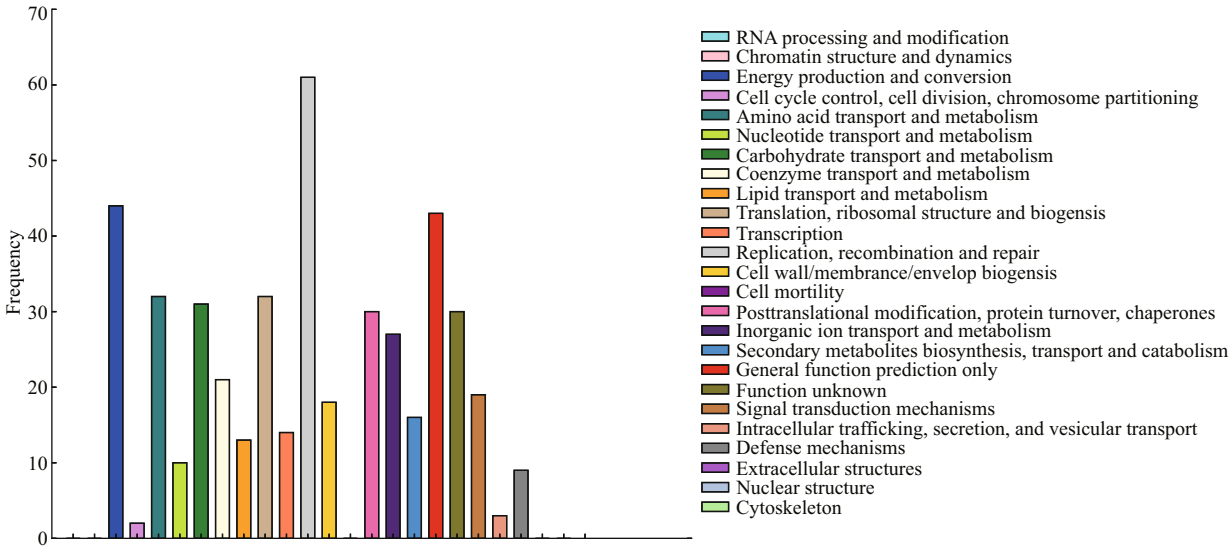

Fig.3 COG classification of all the DEGs

The total of 418 significant DEGs were functionally classified into 25 COG categories.

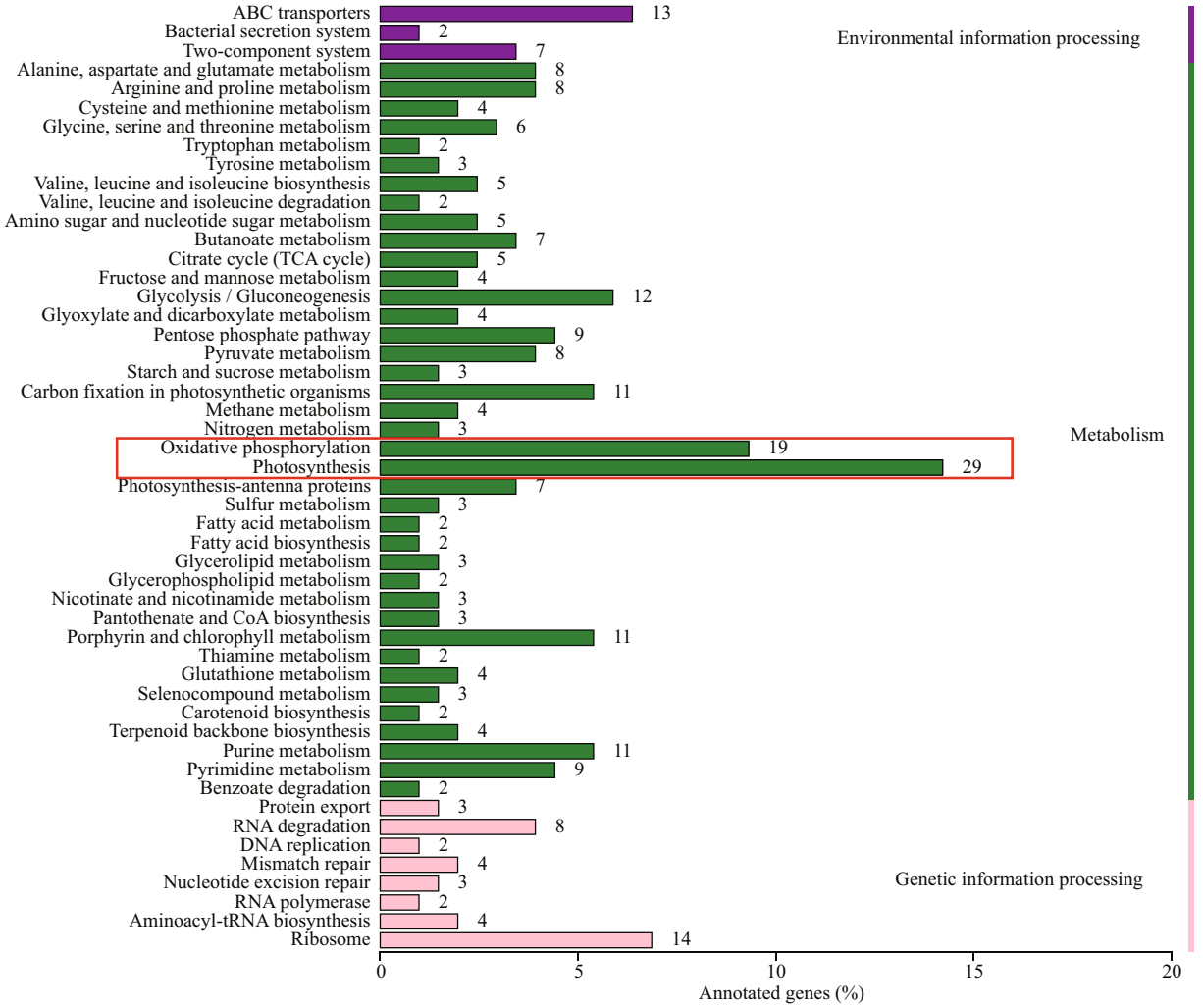

Fig.4 The KEGG pathway classification assigned to the *M. aeruginosa* transcripts after 72-h exposure to $CuSO_4$

KEGG pathways were performed for all sequenced transcripts. The numbers to the right of bars represent the actual number of genes transcribed. The largest number of genes enriched with *Q*-value <0.05 was marked in red box.

Table 5 The genes related to photosynthesis from the transcriptome analysis

Genes ID	$\log_2$ (Cu^{2+}/control)	Regulated	Nr_annotation
MAE_RS14490	-2.654 77	Down	Cytochrome B6
MAE_RS18960	-2.114 35	Down	Photosystem I reaction center subunit XI
MAE_RS00390	-1.924 48	Down	ATP synthase subunit beta
MAE_RS19180	-1.682 75	Down	Photosystem II manganese-stabilizing polypeptide
MAE_RS04545	-1.579 83	Down	Photosystem II protein D1
MAE_RS13940	-1.744 89	Down	Photosystem II reaction center protein Z
MAE_RS14285	-1.948 55	Down	Cytochrome b559 subunit alpha
MAE_RS25860	-3.138 88	Down	MULTISPECIES: photosystem I iron-sulfur center
MAE_RS14280	-2.144 55	Down	MULTISPECIES: cytochrome b559 subunit beta
MAE_RS10170	-2.038 05	Down	Photosystem I reaction center subunit II
MAE_RS04475	-2.067 75	Down	Photosystem II protein D1
MAE_RS21775	-2.031 54	Down	ATP synthase gamma chain
MAE_RS08410	-1.264 89	Down	MULTISPECIES: cytochrome b6-f complex iron-sulfur subunit
MAE_RS00395	-2.631 5	Down	MULTISPECIES: ATP synthase epsilon chain
MAE_RS04750	-1.155 97	Down	Photosystem II protein D1
MAE_RS04610	-1.442 55	Down	Photosystem II protein D1
MAE_RS15785	-1.943 5	Down	Photosystem II extrinsic protein
MAE_RS21745	-3.525 97	Down	MULTISPECIES: ATP synthase subunit a
MAE_RS25355	-2.395 15	Down	Photosystem II protein D1
MAE_RS08415	-1.243 67	Down	Apocytochrome f
MAE_RS23630	-3.141 7	Down	Photosystem II reaction center Psb28 protein
MAE_RS05215	-2.007 75	Down	Cytochrome C & apos
MAE_RS20540	-1.792 59	Down	MULTISPECIES: photosystem I reaction center subunit III
MAE_RS15800	-1.498 81	Down	Ferredoxin
MAE_RS07875	-1.849 91	Down	Photosystem II D2
MAE_RS10240	-1.632 07	Down	Photosystem II protein
MAE_RS05555	-1.196 21	Down	Ferredoxin-NADP reductase
MAE_RS14275	-1.980 11	Down	Photosystem II CP47 chlorophyll apoprotein
MAE_RS21765	-1.470 92	Down	ATP synthase subunit delta

3.8 The genes related to photosynthesis and oxidative phosphorylation based on KEGG enrichment

In the present study, 29 genes related to photosynthesis (Table 5) and 17 genes related to oxidative phosphorylation (Table 6) were identified. Among 29 down-regulated photosynthesis genes, most genes were involved in photosystem I (PS I) (4 genes) and photosystem II (PS II) (12 genes). Among 17 genes related to oxidative phosphorylation, the *ndh* series genes (including that coding for NADH dehydrogenase) were the most prevalent.

3.9 Validation of RNA-Seq by real-time PCR

Real-time PCR was used to validate the mRNA expression of eight genes (from those included in Tables 5 and 6). Regardless of the Cu^{2+} treatment, the mRNAs of *rbcL*, *psbA*, *psbD*, *psaC*, *ATPb*, and *ndhC* were all significantly down-regulated compared to the control. While, the mRNAs of *Cyt-c* and *SDH* were significantly up-regulated compared to the control. Hence, the expression patterns were similar to those in the transcriptome (Fig.5).

3.10 RT-PCR analysis of eight genes during periods of Cu^{2+} stress

In *M. aeruginosa*, over the entire 72 h of Cu^{2+} stress, the 8 validated genes displayed various expression patterns, and the transcription of *rbcL*, *psbA*, *psbD*, *psaC*, *ATPb*, and *ndhC* were all decreased

Table 6 The genes related to oxidative phosphorylation identified by the transcriptome analysis

Genes ID	$\log_2$ (Cu^{2+}/control)	Regulated	Nr_annotation
MAE_RS00390	-1.92	Down	ATP synthase subunit beta
MAE_RS00395	-2.63	Down	MULTISPECIES: ATP synthase epsilon chain
MAE_RS00480	1.33	Up	NADH dehydrogenase
MAE_RS05180	-2.34	Down	MULTISPECIES: NAD(P)H-quinone oxidoreductase subunit 3
MAE_RS05185	-2.75	Down	NAD(P)H-quinone oxidoreductase subunit K
MAE_RS05190	-2.93	Down	NAD(P)H-quinone oxidoreductase subunit J
MAE_RS09985	3.38	Up	Protoheme IX farnesyltransferase
MAE_RS09990	6.18	Up	Cytochrome C oxidase subunit I
MAE_RS13990	-1.15	Down	Oxidoreductase
MAE_RS21745	-3.52	Down	MULTISPECIES: ATP synthase subunit a
MAE_RS21765	-1.47	Down	ATP synthase subunit delta
MAE_RS21775	-2.03	Down	ATP synthase gamma chain
MAE_RS22725	-2.24	Down	NAD(P)H-quinone oxidoreductase subunit H
MAE_RS24330	-1.63	Down	NAD(P)H-quinone oxidoreductase subunit 2
MAE_RS24490	3.83	Up	Succinate dehydrogenase
MAE_RS24580	-2.28	Down	NAD(P)H-quinone oxidoreductase subunit I
MAE_RS24585	-2.00	Down	MULTISPECIES: NAD(P)H-quinone oxidoreductase subunit 1

at the tested time points. However, the transcription of *Cyt-c* and *SDH* were enhanced during the periods of Cu^{2+} stress (Fig.6).

4 DISCUSSION

There are few related reports on the influence of chemical reagents on *M. aeruginosa*, and most of these papers are focused on the analysis of physiological parameters such as algae mortality, chlorophyll content and antioxidant enzymes (Hong et al., 2008; Lu et al., 2014; Chen et al., 2015). In this study, we investigated the effect of Cu^{2+} on the above physiological parameters of *M. aeruginosa*, and on its transcriptome too.

Copper is a micronutrient essential for the growth of organisms by participating in many physiological processes, such as the photosynthetic and respiratory electron-transport chains, the C and N metabolism, hormone perception, cell wall metabolism, and oxidative stress protection. However, Cu^{2+} poisoning can occur if organisms take excessive amounts of Cu^{2+} (Garcia-Molina et al., 2011). In the present study, Cu^{2+} content in *M. aeruginosa* increased by 1 356% after Cu^{2+} exposure for 72 h, with Chl *a* content in *M. aeruginosa* sharply decreasing and antioxidant enzymes (SOD, CAT and POD) all increasing. The results indicate that the Cu^{2+} concentration in BG-11 medium was above the

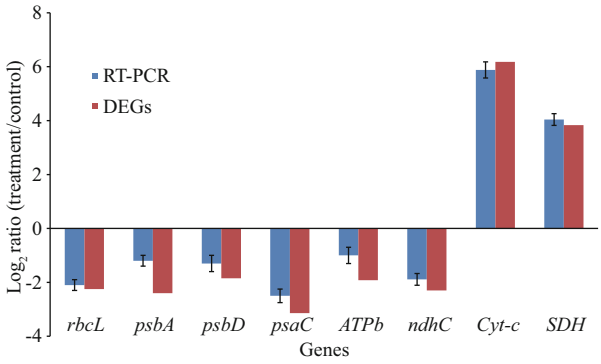

Fig.5 Validation of transcriptome data by real-time PCR of six differentially expressed genes

Chosen from Tables 5 and 6. Data are means±SE (n=3).

M. aeruginosa growth needs, and led to an oxidative stress in *M. aeruginosa*. Similar results were reported by Lu et al. (2015) and Wu et al. (2017).

Photosynthesis is one of the most important activities in cyanobacterial cells and is also regarded as a major target of allelopathic substances. In this study, the F_v/F_m ratio indicates the efficiency of photosynthetic apparatus (Shao et al., 2011) by representing the maximum quantum efficiency of PSII photochemistry (Baker, 2008). We find the F_v/F_m value was decreased in the Cu^{2+} treatment with increasing exposure time, indicating Cu^{2+} was responsible for the inhibition of photosynthesis. Similar results were reported by Boucher and

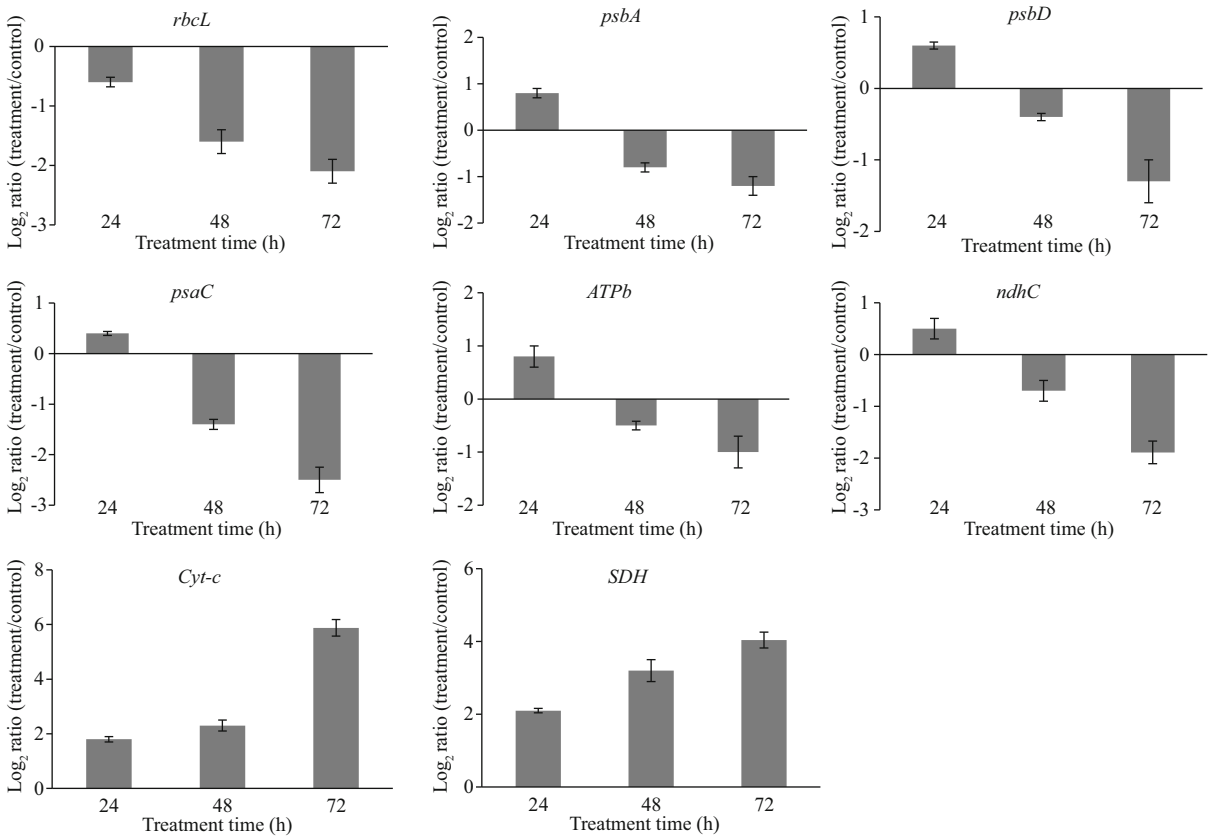

Fig.6 RT-PCR analysis of 8 genes (*rbcL*, *psbA*, *psbD*, *psaC*, *ATPb*, *ndhC*, *Cyt-c*, and *SDH*) during periods of Cu^{2+} stress (24, 48, 72 h) in *M. aeruginosa*

The RT-PCR results are the means±SE (n=3).

Carpentier (1999) and Chen et al. (2015) using different metals (e.g. Hg^{2+}, Pb^{2+}, and Na^{2+}).

In order to understand the potential regulatory mechanisms of Cu^{2+} toxicity stress in *M. aeruginosa*, RNA-seq technology was used as an important tool for global analysis of gene discovery and molecular mechanisms under environmental stress (Wang et al., 2017). With RNA-seq technology, we sequenced the transcriptomes of Cu^{2+}-treated and untreated *M. aeruginosa*, respectively, and obtained 6 646 725 and 7 880 291 clean reads matched to one or more public databases. According to the results of GO classification in our study, most DEGs were involved in the important category of biological process, such as metabolic process, cellular process and single-organism process. These findings are similar to the result of Wang et al. (2016). However, in another study, 'metallochaperone activity' and 'translation regulator activity' were the most representative (Gai et al., 2012), two categories containing the fewest genes in the study presented here. This difference may be on due to different species used. In addition, the second explanation for functional class differences may be better gene sequence information, existing a series of low-abundance transcripts, being provided by Illumina sequencing platform (this study) than 454 GS-FLX platform (Gai et al., 2012).

In addition to GO analysis, assignments of COG were performed to reveal the diversity of the assembled transcripts while reflecting the global landscape of the transcriptome (Wu et al., 2014; Wang et al., 2016). In this paper, a total of 418 DEGs were obtained, of which 25 have functional definitions. 'Replication, recombination and repair', 'energy production and conversion', and 'general function prediction only' were the largest three groups of transcripts. Hanawalt (2007) reported that the replication and maintenance of the genome are absolute requirements for life. A cell must duplicate its entire complement of DNA with astonishing precision in the face of a barrage of deleterious endogenous and environmental genotoxic agents, as well as the intrinsic chemical instability of the DNA molecule itself. In our study, many DEGs might still need to be functionally verified in our findings, as

nucleotide sequencing and protein metabolism of *M. aeruginosa* could be active.

The KEGG pathway database involves a systematic analysis of inner-cell metabolic pathways and functions of gene products (Wang et al., 2016). In this study, KEGG pathway analysis annotated about half of DEGs, whereas NR database annotated all DEGs identified. Similar results were reported by Wang et al. (2016), in which more DEGs were identified in NR database than other database. However, KEGG pathway database is the widely used database to find enriched pathway. KEGG pathway database is a valuable collection of manually constructed maps representing the current knowledge on the molecular interaction and reaction networks for metabolism, processing of genetic and environmental information, cellular processes, etc. Moreover, KEGG (as a part of a system biology approach) can be considered as a virtual biological system including various types of information essential for the recreation of a living creature (Kanehisa and Goto, 2000). The results of this study indicate that most affected metabolic pathways were in photosynthesis and oxidative phosphorylation. Among the down-regulated photosynthesis genes, most genes were involved in photosystem I (PS I) and photosystem II (PS II). Zou et al. (2015) found PS I and PS II in photosynthetic organisms are sensitive to environmental variation. Our transcriptome and RT-PCR results proved that core proteins expressions in the PS I and PS II reaction centers was depressed in response to Cu^{2+} stress. These findings are consistent with Lu et al. (2014), who examined the effect of the epigallocatechin-3-gallate treatment on the gene expression of *M. aeruginosa*.

Through the research, the 29 genes related to photosynthesis can be considered a target for the subsequent Cu^{2+} stress analysis. Among 16 genes involved in PS I and PS II is the *psbA* gene that encodes D1 protein as the key protein in the PS II reaction center. The D1 protein is involved in the PSII repair cycle by binding to all the redox active components, while participating in the PS II repair cycle with degrading and resynthesizing in a multistep process (Leu et al., 2002; Leng et al., 2015). As Mulo et al. (2012) reported, in this study the time-dependent down regulation of *psbA* transcription can impede electron transport and suppress the electron transport activity in PSII. The rubisco protein is encoded by the *rbcL* gene and acts as a key protein in the light-independent reactions, involved in the carbon assimilation process (Mulo et al., 2012; Chen et al., 2015). The experimental results reveal that electron transport, energy conversion and photosynthesis of *M. aeruginosa* are necessary for CO_2 fixation, but they are inhibited under Cu^{2+} conditions. In summary, the hindrance of carbon assimilation under Cu^{2+} stress suppressed the photosynthesis of *M. aeruginosa*. Interestingly, 12 differentially expressed transcripts linked to PS II compared to only 4 in PS I, demonstrating that PS II was more sensitive than PSI to Cu^{2+} toxicity stress, similar results were reported by Boucher and Carpentier (1999) and Leng et al. (2015).

Oxidative phosphorylation is a metabolic pathway in which cells use enzymes to oxidize nutrients, and the energy released during oxidation of the substance in the body provides the coupling reaction process for the synthesis of ATP from ADP and inorganic phosphate (Powell and Somero, 1986). This metabolic pathway was taken place in the mitochondria and releases energy more efficiently than alternative fermentation processes such as anaerobic glycolysis, so that oxidative phosphorylation process is present in most aerobic organisms (Guo et al., 2016b). Although oxidative phosphorylation pathway is a primary part of the metabolism, it produces ROS, which in turn leads to the proliferation of radicals, destroying cells and causing aging and disease (Kuno et al., 1985; Powell and Somero, 1986). In the present study, ROS concentration and antioxidant enzyme activity (e.g. SOD, CAT) increased in *M. aeruginosa* after 72 h Cu^{2+} exposure (as above), with excess ROS causing cell damages. Leng et al. (2015) reported NADPH oxidase has been suggested to play a crucial role in the generation and accumulation of ROS in cyanobacteria under stress conditions.

It was worth nothing that the 17 differentially expressed genes related to oxidative phosphorylation could be used as the targets genes for oxidative analysis. Among these genes, *ndh* series genes represented the largest proportion. The *ndh* could encode NADH dehydrogenase, a main component of the electron transport chain that transfers electrons from NADH to coenzyme Q (Lu et al., 2014). In this study, the expression of *ndhC* gene was time-dependent decreased, which might give rise to serious damage to the cells. Furthermore, the ATP synthase genes were also time-dependent down (such as *ATPb*). Lu et al. (2014) pointed out that the down-regulation of photosynthesis and ATP synthase were markers of the photoinhibition.

5 CONCLUSION

This study discovered numerous genes that were differentially expressed between the control and Cu^{2+}-toxicity-stressed *M. aeruginosa*. Transcriptome analysis results indicate that exogenous Cu^{2+} regulated numerous genes related to photosynthesis and oxidative phosphorylation. The photosynthesis in *M. aeruginosa* was hindered by changing carbon assimilation under Cu^{2+} stress. Our research will help understand and explain the complex molecular mechanisms of *M. aeruginosa* responses to Cu^{2+} toxicity stress.

6 DATA AVAILABILITY STATEMENT

The datasets generated during the current study are available from the corresponding author on reasonable request.

7 ACKNOWLEDGEMENT

We thank Genepioneer Biotechnologies (Nanjing, China) for the assistance in analysis of the RNA-seq data.

References

Anders S, Huber W. 2010. Differential expression analysis for sequence count data. *Genome Biology*, **11**(10): R106.

Baker N R. 2008. Chlorophyll fluorescence: a probe of photosynthesis in vivo. *Annual Review of Plant Biology*, **59**: 89-113.

Barrington D J, Ghadouani A. 2008. Application of hydrogen peroxide for the removal of toxic cyanobacteria and other phytoplankton from wastewater. *Environmental Science & Technology*, **42**(23): 8 916-8 921.

Boucher N, Carpentier R. 1999. Hg^{2+}, Cu^{2+}, and Pb^{2+}-induced changes in photosystem II photochemical yield and energy storage in isolated thylakoid membranes: a study using simultaneous fluorescence and photoacoustic measurements. *Photosynthesis Research*, **59**(2-3): 167-174.

Bradford M M. 1976. A rapid and sensitive method for the quantitation of microgram quantities of protein utilizing the principle of protein-dye binding. *Analytical Biochemistry*, **72**(1-2): 248-254.

Chen L, Mao F J, Kirumba G C, Jiang C, Manefield M, He Y L. 2015. Changes in metabolites, antioxidant system, and gene expression in *Microcystis aeruginosa* under sodium chloride stress. *Ecotoxicology and Environmental Safety*, **122**: 126-135.

Conesa A, Götz S, García-Gómez J M, Terol J, Talón M, Robles M. 2005. Blast2GO: a universal tool for annotation, visualization and analysis in functional genomics research. *Bioinformatics*, **21**(18): 3 674-3 676.

Foster S, Thomson D, Maher W. 2008. Uptake and metabolism of arsenate by anexic cultures of the microalgae *Dunaliella tertiolecta* and *Phaeodactylum tricornutum*. *Marine Chemistry*, **108**(3-4): 172-183.

Gai S P, Zhang Y X, Mu P, Liu C Y, Liu S, Dong L, Zheng G S. 2012. Transcriptome analysis of tree peony during chilling requirement fulfillment: assembling, annotation and markers discovering. *Gene*, **497**(2): 256-262.

Garcia-Molina A, Andrés-Colás N, Perea-García A, Del Valle-Tascón S, Peñarrubia L, Puig S. 2011. The intracellular Arabidopsis COPT5 transport protein is required for photosynthetic electron transport under severe copper deficiency. *Plant Journal*, **65**(6): 848-860.

Gera A, Alcoverro T, Mascaró O, Pérez M, Romero J. 2012. Exploring the utility of *Posidonia oceanica* chlorophyll fluorescence as an indicator of water quality within the European Water Framework Directive. *Environmental Monitoring and Assessment*, **184**(6): 3 675-3 686.

Gui D, Liu W B, Shao X P, Xu W N. 2010. Effects of different dietary levels of cottonseed meal protein hydrolysate on growth, digestibility, body composition and serum biochemical indices in crucian carp (*Carassius auratus gibelio*). *Animal Feed Science and Technology*, **156**(3-4): 112-120.

Guo R Y, Lim W A, Ki J S. 2016a. Genome-wide analysis of transcription and photosynthesis inhibition in the harmful dinoflagellate *Prorocentrum minimum* in response to the biocide copper sulfate. *Harmful Algae*, **57**: 27-38.

Guo R Y, Wang H, Suh Y S, Ki J S. 2016b. Transcriptomic profiles reveal the genome-wide responses of the harmful dinoflagellate *Cochlodinium polykrikoides* when exposed to the algicide copper sulfate. *BMC Genomics*, **17**: 29.

Hadjoudja S, Vignoles C, Deluchat V, Lenain JF, Le Jeune AH, Baudu M. 2009. Short term copper toxicity on *Microcystis aeruginosa* and *Chlorella vulgaris* using flow cytometry. *Aquatic Toxicology*, **94**(4): 255-264.

Hanawalt P C. 2007. Paradigms for the Three Rs: DNA replication, recombination, and repair. *Molecular Cell*, **28**(5): 702-707.

Hong Y, Hu H Y, Xie X, Li F M. 2008. Responses of enzymatic antioxidants and non-enzymatic antioxidants in the cyanobacterium *Microcystis aeruginosa* to the allelochemical ethyl 2-methyl acetoacetate (EMA) isolated from reed (*Phragmites communis*). *Journal of Plant Physiology*, **165**(12): 1 264-1 273.

Hrudey S, Burch M D, Drikas M, Gregory R. 1999. Remedial measures. *In*: Chorus I, Bartram J eds. Toxic Cyanobacteria in Water: A Guide to Their Public Health Consequences, Monitoring, and Management. E & FN Spon, New York. p.275-312.

Kanehisa M, Goto S. 2000. KEGG: Kyoto encyclopedia of genes and genomes. *Nucleic Acids Research*, **28**(1): 27-30.

Kaneko T, Nakajima N, Okamoto S, Suzuki I, Tanabe Y, Tamaoki M, Nakamura Y, Kasai F, Watanabe A, Kawashima K, Kishida Y, Ono A, Shimizu Y, Takahashi C, Minami C, Fujishiro T, Kohara M, Katoh M, Nakazaki

N, Nakayama S, Yamada M, Tabata S, Watanabe MM. 2007. Complete genomic structure of the bloom-forming toxic cyanobacterium *Microcystis aeruginosa* NIES-843. *DNA Research*, **14**(6): 247-256.

Kuno S, Bacher A, Simon H. 1985. Structure of enoate reductase from a *Clostridium tyrobutyricum* (*C. spec*. La1). *Biological Chemistry Hoppe-Seyler*, **366**(5): 463-472.

Leng X P, Jia H F, Sun X, Shangguan L F, Mu Q, Wang B J, Fang J G. 2015. Comparative transcriptome analysis of grapevine in response to copper stress. *Scientific Reports*, **5**: 17749.

Leu E, Krieger-Liszkay A, Goussias C, Gross E M. 2002. Polyphenolic allelochemicals from the aquatic angiosperm *Myriophyllum spicatum* inhibit photosystem II. *Plant Physiology*, **130**(4): 2 011-2 018.

Lu L, Wu Y X, Ding H J, Zhang W H. 2015. The combined and second exposure effect of copper (II) and chlortetracycline on fresh water algae, *Chlorella pyrenoidosa* and *Microcystis aeruginosa*. *Environmental Toxicology and Pharmacology*, **40**(1): 140-148.

Lu Y P, Wang J, Yu Y, Shi L M, Kong F X. 2014. Changes in the physiology and gene expression of *Microcystis aeruginosa* under EGCG stress. *Chemosphere*, **117**: 164-169.

Mulo P, Sakurai I, Aro E M. 2012. Strategies for *psbA* gene expression in cyanobacteria, green algae and higher plants: from transcription to PSII repair. *Biochimica et Biophysica Acta*, **1817**(1): 247-257.

Ohkawa H, Ohishi N, Yagi K. 1979. Assay for lipid peroxides in animal tissues by thiobarbituric acid reaction. *Analytical Biochemistry*, **95**(2): 351-358.

Otten T G, Paerl H W. 2015. Health effects of toxic cyanobacteria in U.S. drinking and recreational waters: our current understanding and proposed direction. *Current Environmental Health Reports*, **2**(1): 75-84.

Powell M A, Somero G N. 1986. Hydrogen sulfide oxidation is coupled to oxidative phosphorylation in mitochondria of *Solemya reidi*. *Science*, **233**(4763): 563-566.

Rascioa N, Navari-Izzo F. 2011. Heavy metal hyperaccumulating plants: how and why do they do it? And what makes them so interesting? *Plant Science*, **180**(2): 169-181.

Shao J H, Xu Y, Wang Z J, Jiang Y G, Yu G L, Peng X, Li R H. 2011. Elucidating the toxicity targets of β-ionone on photosynthetic system of *Microcystis aeruginosa* NIES-843 (Cyanobacteria). *Aquatic Toxicology*, **104**(1-2): 48-55.

Trapnell C, Williams B A, Pertea G, Mortazavi A, Kwan G, van Baren M J, Salzberg S L, Wold B J, Pachter L. 2010. Transcript assembly and quantification by RNA-Seq reveals unannotated transcripts and isoform switching during cell differentiation. *Nature Biotechnology*, **28**(5): 511-515.

Tsai K P. 2015. Effects of two copper compounds on *Microcystis aeruginosa* cell density, membrane integrity, and microcystin release. *Ecotoxicology and Environmental Safety*, **120**: 428-435.

Wang T, Long X H, Chen X Y, Liu Y R, Liu Z P, Han S Q, Yan S H. 2017. Integrated transcriptome, proteome and physiology analysis of *Epinephelus coioides* after exposure to copper nanoparticles or copper sulfate. *Nanotoxicology*, **11**(2): 236-246.

Wang X H, Hui F, Yang Y C, Yang S H. 2018. Deep sequencing and transcriptome analysis to identify genes related to biosynthesis of aristolochic acid in *Asarum heterotropoides*. *Scientific Reports*, **8**: 17 850.

Wang Y J, Dong C L, Xue Z Y, Jin Q J, Xu Y C. 2016. *De novo* transcriptome sequencing and discovery of genes related to copper tolerance in *Paeonia ostii*. *Gene*, **576**(1): 126-135.

Wu H M, Wei G J, Tan X, Li L, Li M. 2017. Species-dependent variation in sensitivity of *Microcystis* species to copper sulfate: implication in algal toxicity of copper and controls of blooms. *Scientific Reports*, **7**: 40 393.

Wu H X, Jia H M, Ma X W, Wang S B, Yao Q S, Xu W T, Zhou Y G, Gao Z S, Zhan R L. 2014. Transcriptome and proteomic analysis of mango (*Mangifera indica* Linn) fruits. *Journal of Proteomics*, **105**: 19-30.

Zhang S L, Xing K Z, Zhou Y. 2007. The acute toxicity of copper ion on alga *Microcystis aeruginosa*. *Fisheries Science*, **26**(6): 323-326. (in Chinese with English abstract)

Zhou S Q, Shao Y S, Gao N Y, Deng Y, Qiao J L, Ou H S, Deng J. 2013. Effects of different algaecides on the photosynthetic capacity, cell integrity and microcystin-LR release of *Microcystis aeruginosa*. *Science of the Total Environment*, **463-464**: 111-119.

Zou H X, Pang Q Y, Zhang A Q, Lin L D, Li N, Yan X F. 2015. Excess copper induced proteomic changes in the marine brown algae *Sargassum fusiforme*. *Ecotoxicology and Environmental Safety*, **111**: 271-280.